Journal of Applied Polymer Science

Modification of structural, thermal, and electrical properties of PVA by addition of silicon carbide nanocrystals

Isha Saini,[1] Annu Sharma,[1] Jyoti Rozra,[1] Rajnish Dhiman,[2] Sanjeev Aggarwal,[1] Pawan K. Sharma[3]

[1]Department of Physics, Kurukshetra University, Kurukshetra 136 119, India

[2]Department of Chemical Engineering, Biotechnology and Environmental Technology, University of Southern Denmark, Campusvej 55, DK-5230 Odense M, Denmark

[3]Department of Chemistry, Kurukshetra University, Kurukshetra 136 119, India

Correspondence to: A. Sharma (E-mail: talk2annu@gmail.com)

ABSTRACT: SiC-PVA nanocomposite films, synthesized using solution-casting technique were structurally characterized using X-ray diffraction (XRD), Fourier transform infrared spectroscopy (FTIR) and Raman spectroscopy. Morphological studies of the SiC-PVA nanocomposite films were carried out using Transmission electron microscopy (TEM) and Scanning electron microscopy (SEM). TEM analysis confirms that the size of SiC nanocrystals present in PVA matrix are 23 ± 9 nm, which is consistent with size calculated using XRD. SiC-PVA nanocomposite films were further characterized for their thermal and electrical properties. Thermogravimetric/differential thermal analysis (TG/DTA) indicates that the char yield of nanocomposite films containing 3 wt % SiC nanocrystal is ~30% more than PVA. This increase in char yield is an indication of the potency of flame retardation of SiC-PVA nanocomposite films. *I-V* analysis reveals that Schottky mechanism is the dominant conduction mechanism which is responsible for the increase in conductivity of PVA with the addition of SiC nanocrystals. © 2015 Wiley Periodicals, Inc. J. Appl. Polym. Sci. **2015**, *132*, 42464.

KEYWORDS: charge transport; nanostructured polymers; thermal properties

Received 21 December 2014; accepted 4 May 2015

DOI: 10.1002/app.42464

INTRODUCTION

In recent past, nanocomposite materials consisting of dispersed semiconducting nanoparticles such as SiC, ZnO, CdS, etc. in a polymer matrix have attracted substantial scientific and technological interest in materials research as they display superior structural, thermal, electrical, and electrochemical properties because of the high surface-to-volume ratio of nanometer scale reinforcing fillers embedded in the matrix in comparison to the conventional particle reinforced composites.[1–3] Many of these properties can be controlled by altering the nature, size, shape, and distribution of the nanoparticles within the polymer matrix, hence offering immense opportunities for designing materials with tunable properties.

SiC nanoparticles seem to be an appropriate candidate for synthesis of such nanocomposites as it has good thermal stability, resistance toward oxidation, chemical inertness, and mechanical hardness; moreover, it is versatile from structural considerations (more than 250 polytypes), electronic behavior (a variable gap from 2.4 to 3.3 eV), as well as the photorefractive response. When these nanoparticles are embedded in suitable matrices, promising new potentialities such as charge transfer, nonlinear optics, and electro-optics are anticipated.[4,5] SiC is also attracted increasing interest due to its desirable properties for potential applications as semiconductor devices.[6] When micron-sized SiC particles are added in a matrix and the particles have some level of contact with each other, it has been observed that the conductivity of the composite increases.[7] Thus it is logical to assume that incorporation of SiC nanoparticles into a polymer matrix could further enhance the properties of the polymer as a nanocomposite material.

Furthermore, an improvement in the flammability properties of polymers has been achieved with addition of SiC nanoparticles as it retains its strength at high temperatures, which could serve as an alternative to conventional flame retardants.[8]

There are quite a few reports describing the improvement in optical, structural, thermal, and electrical properties of SiC-based nanocomposites. Guo *et al.* fabricated polyurethane-SiC nanocomposites by a facile surface-initiated-polymerization (SIP) method and resulting nanocomposites has enhanced thermal stability and improved mechanical properties.[9] Studies carried out by Chisholm *et al.* on SiC-epoxy nanocomposites have revealed improved thermal properties due to the increase in cross-linking of epoxy resin in the presence of 1.5 wt % SiC nanoparticles.[10] Tkaczyk reported a giant increase in current

with the addition 5 wt % SiC nanocrystals in Polibutadien matrix.[11] Dash *et al.* synthesized Starch-SiC bionanocomposites by varying the concentration of SiC nanoparticles from 0 to 10 wt % and have shown improvement in char yield and remarkable reduction in oxygen permeability due to dispersion of SiC in the starch matrix.[12]

Among the synthetic polymers, poly(vinyl alcohol) (PVA) is hydrophilic and biodegradable polymer, which has large technological applications. It has good solubility in water due to the formation of strong hydrogen bond between the functional group of polymer and the water molecules.[13] Furthermore, it has good film forming ability when the films are prepared by solution casting technique. The films of the PVA are highly optically transparent, which makes it suitable for surface coating of the solid state optoelectronic devices and other multifunctional materials. The main drawback of this hydrophilic polymer is its poor mechanical and thermal stability.

Despite being very tough, highly thermally stable with many other extraordinary properties, the potential of SiC nanoparticles as reinforcing filler for the improvement of mechanical, thermal, or electrical properties of PVA are seldom reported. Vivekchand *et al.* reported an increase in the elastic modulus of PVA with addition of only 0.8 vol % of SiC nanowires.[14] Zhang *et al.* studied the influence of PVA as a binder on the zeta potential and rheological properties of SiC slurries.[15] There are hardly any reports in literature describing the structural, thermal and electrical characterization of SiC-PVA nanocomposites.

Thus in the present study the compatibility and interactions between SiC nanocrystals and PVA matrix as well as the effects of SiC nanocrystals on the structural, thermal and electrical properties of PVA were investigated by X-ray diffraction (XRD), scanning electronic microscopy (SEM), transmission electron microscopy (TEM), FTIR, Raman spectroscopy, thermogravimetry analysis (TGA), differential thermal analysis (DTA), and I-V measurements.

EXPERIMENTAL

Materials

Analytical reagent grade poly(vinyl alcohol) PVA (Molecular Weight = 1,25,000 g/mol) obtained from Ranbaxy was used as received. Nanoporous SiC was synthesized by reacting nanoporous carbon black (Vulcan® XC-72) having particle size of 25–35 nm, with SiO vapors which were generated *in situ* by heating a uniform 1 : 1 molar mixture of silicon and silica powder at 1450°C. The carbon black was placed next (downstreams) to this mixture in the alumina crucible. The furnace was heated to a temperature of 1450°C for 12–15 h in an argon flow of 250–300 mL/min. Detailed mechanism has been explained in Dhiman *et al.*,[16] which is adopted from Dhiman *et al.*,[17] where the charcoal obtained from wood had been used as the source of carbon.

Nanocomposite Preparation

For the preparation of SiC-PVA nanocomposite, appropriate amount of PVA was dissolved in distilled water. The solution was stirred until the polymer completely dissolved and formed a clear viscous solution. Varying concentrations of SiC nanocrystals were dissolved in distilled water in separate beakers under high ultrasonication for 30 min. These solutions were slowly added to the viscous polymer solution to obtain SiC-PVA nanocomposites films having 1, 2, and 3 wt % of SiC nanocrystals. For uniform dispersion of nanocrystals into PVA matrix ultrasonication was carried out for another 30 min. This procedure was carried out at room temperature and under ambient pressure. The resulting solutions so obtained were poured in Petri dishes and left for a period of 4–5 days for solidification. The resulting nanocomposite films were then peeled off for further characterization.

Characterization

X-ray diffraction measurements were carried out on a Mini Flex II Rigaku model diffractometer using CuK_α radiation ($\lambda = 0.154$ nm) in the wide angle region from 20° to 80°. For TEM investigations, a small drop of the suspension of nanocomposite film was put on a carbon-coated copper grid. After drying the grid, TEM was carried out employing Hitachi-H7500 electron microscope operating at 80 kV accelerating voltage. SEM measurements were carried out using LEO 435 VP scanning electron microscope. FTIR (Perkin-Elmer 577) and Raman spectrometer (using the 532 nm wavelength laser with resolution 3–5 nm) were used to investigate the fundamental vibrations of the nanocomposite films, in the range 4000–400 cm^{-1}.

After structural characterization, these nanocomposites were thermally characterized using Perkin Elmer Diamond TG/DTA analyzer at a heating rate of 10°C/min, from room temperature up to 700°C, in air atmosphere at a flow of 20 mL/min. Current-Voltage (I-V) behavior was studied using four probe Keithley (6517A) electrometer at room temperature. For I-V measurements SiC–PVA nanocomposites films of 5 cm diameter were laid between the Keithley 8009 resistivity text fixture and a testing voltage of 100 V was applied.

RESULTS AND DISCUSSION

Structural Analysis

Figure 1 displays the XRD pattern of PVA (curve a) and SiC-PVA nanocomposite films, containing 1, 2 and 3 wt % SiC nanocrystals (curves b-d). XRD pattern of SiC-PVA nanocomposite films Figure 1 (curves b-d) shows a major peak at 2θ value of 35.82° which corresponds to (111) plane of SiC nanocrystals and increases with increasing concentration of SiC nanocrystals in PVA matrix. Diffraction pattern of nanocomposite film containing 3 wt % SiC nanocrystals, show minor peaks at 2θ values of 41.61°, 60.30°, and 72.04° which corresponds to (200), (220), and (311) planes of SiC nanocrystals and are consistent with the peaks of standard SiC (standard JCPDS file PDF No. 29–1129).[18–20] There is a low intensity peak marked with SF near to the highest intensity peak and is assumed to be due to stacking faults created during the formation of SiC nanocrystals.[16]

XRD pattern was used to calculate the average size of SiC nanocrystals from the full width at half-maximum (FWHM) of the major peak, using the Debye-Scherer equation,[20]

$$D = 0.9\lambda/\beta\cos\theta \quad (1)$$

where λ (= 0.154 nm) is the wavelength of the CuK_α radiation source, β is the full width at half maximum in radians, and θ is

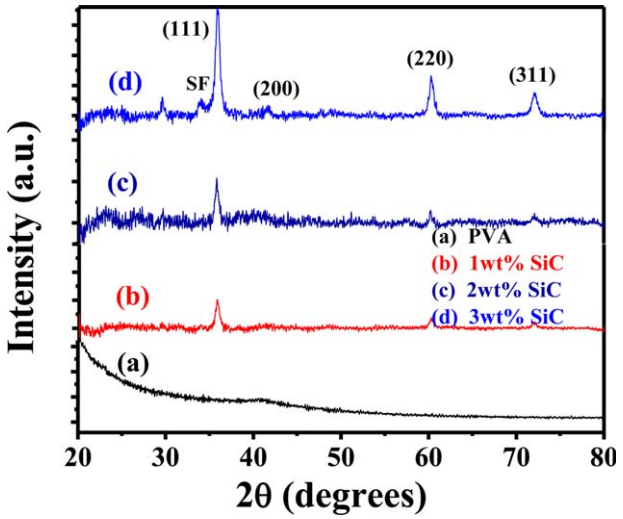

Figure 1. XRD spectrum of (a) PVA and SiC-PVA nanocomposite film containing (b) 1 wt % (c) 2 wt % (d) 3 wt % SiC nanocrystals. [Color figure can be viewed in the online issue, which is available at wileyonlinelibrary.com.]

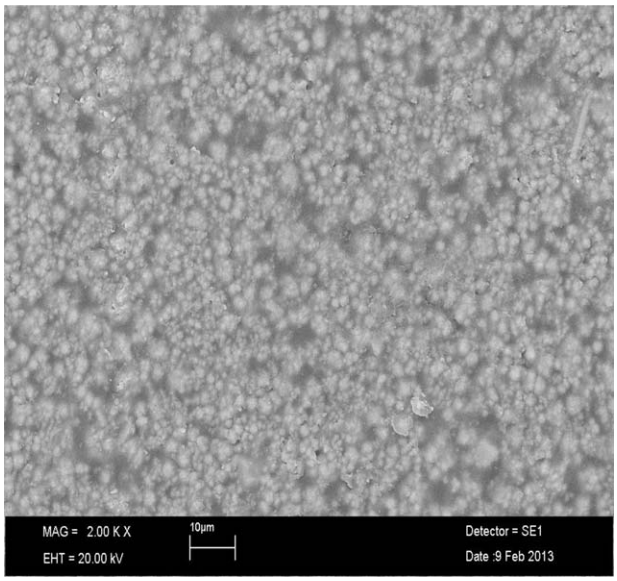

Figure 3. SEM images of SiC-PVA nanocomposite film.

the angle between the incident ray and the scattering planes. Interplanar distance (d) between the crystal planes was determined using the formula,[21]

$$d = n\lambda/2\sin\theta \quad (2)$$

where n is the order of reflection, which may be any integer (1, 2, 3, . . .). The value of interplanar spacing at four major peaks corresponding to the (111), (200), (220), and (311) planes comes out to be 2.52 Å, 2.18 Å, 1.54 Å, and 1.31 Å respectively. Size of SiC nanocrystals dispersed in the PVA matrix calculated using eq. (1) from the major peak corresponding to (111) plane comes out to be 16.8 nm.

Figure 2 depicts the TEM micrograph of SiC-PVA nanocomposite film containing 3 wt % SiC nanocrystals. It reveals that the size of SiC nanocrystals within PVA matrix is 23 ± 9 nm which is consistent with the size obtained from XRD. Further TEM micrograph reveal that SiC nanoparticles were not randomly distributed within the matrix, but tended to cluster around white stuctures (polymer) as SiC nanocrystals are hydrophobic in nature. SEM image of nanocomposite film containing 3 wt % SiC nanocrystals is shown in Figure 3. It shows spherical SiC nanocrystals are dispersed in PVA matrix.

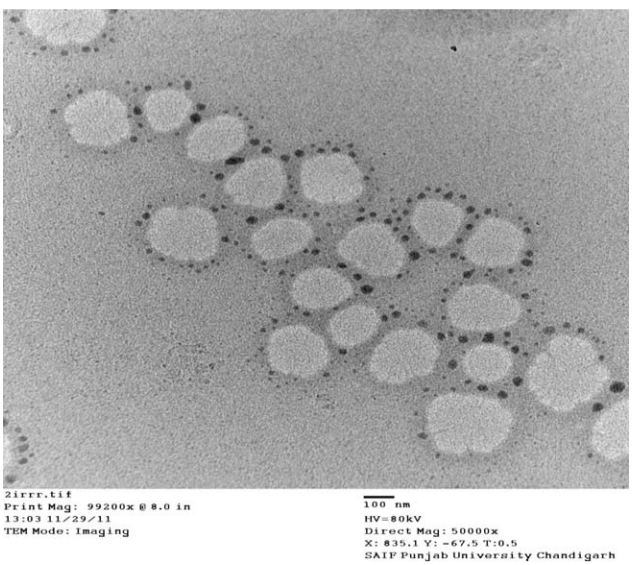

Figure 2. TEM micrograph of SiC-PVA nanocomposite film containing 3 wt % SiC nanocrystals.

Vibrational spectroscopy plays an important role in the elucidation of molecular structure. The vibrational spectrum of a polymer is determined by its conformational state and the nature of the force field. Thus a detailed analysis of FTIR spectra and Raman spectra provides an insight into intramolecular as well as intermolecular interactions.

FTIR spectroscopic studies were carried out on PVA and SiC-PVA nanocomposite films to verify the interaction between PVA and SiC nanocrystals. Figure 4 (curve a) shows all major peaks associated with various functional groups of PVA. The spectrum of PVA Figure 4 (curve a) shows bands at 3358 cm^{-1} attributed to stretching of OH hydroxyl group and at around 2931 cm^{-1} due to the C—H stretching mode of alkyl groups. The bands at 1730 cm^{-1} and 1255 cm^{-1} can be assigned to the residual acetyl group present in PVA.[22] The vibrational bands at 1434 cm^{-1} and 859 cm^{-1} are assigned to CH_2 bending and stretching mode of PVA, respectively. Presence of these vibrational bands confirms the monomer structure of PVA. The assignments of the various bands made in this study are in reasonable agreement with those reported in the literature.[23,24]

In FTIR spectra of SiC-PVA nanocomposite films (curves b-d), the major peaks corresponding to various functional groups of PVA are affected significantly by the addition of SiC nanocrystals in PVA matrix. It can clearly be seen in Figure 4 (curve b-d) that the addition of SiC nanocrystals in PVA matrix results in diminished intensity, broadening of the bands and their displacement towards higher wave numbers. Such a behavior

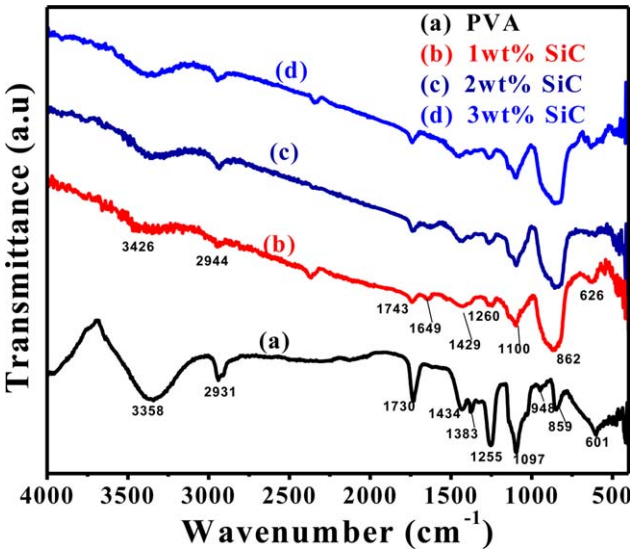

Figure 4. FTIR spectrum of (a) PVA and SiC-PVA nanocomposite films containing (b) 1 wt % (c) 2 wt % (d) 3 wt % SiC nanocrystals. [Color figure can be viewed in the online issue, which is available at wileyonlinelibrary.com.]

signifies the existence of strong interaction between SiC nanocrystals and the PVA matrix. It is reported that bands related to silicon vibrations are mostly found in the region ranging from 800 to 1500 cm^{-1}, therefore, in nanocomposite films, due to the presence of both SiC nanocrystals and PVA components, there is an overlapping of the bands in this region. As a result the band due to C—O stretching movements in PVA at about 1097 cm^{-1} interferes with asymmetric Si—O—Si stretching at around 1046 cm^{-1}; hence, the band shifts towards higher value in nanocomposite films. Another major difference between the spectra of PVA and SiC-PVA nanocomposite films has been observed in the 850 to 950 cm^{-1} region.[22,25] The vibrational band at 862 cm^{-1} in the nanocomposite films is ascribed to the stretching vibrations of the Si—C bonds of the SiC component.[26] Which is in line with an earlier observation in the absorption spectra of a SiO_2 sample with SiC nanocrystal inclusions.[27]

Raman Spectra of PVA and SiC-PVA nanocomposite film is shown in Figure 5(A). The main vibrations in the PVA matrix have been ascribed as follows: bending of C—C—H and C—C bonds (854 and 918 cm^{-1}); stretching of C—O and C—C bonds (1117 and 1226 cm^{-1}); stretching of C—H and bending vibrations of O—H bonds (1362 cm^{-1}); bending of C—H and C—O—H bonds (1462 cm^{-1}) and C—H stretching (2920 cm^{-1}).[28]

After the addition of SiC nanocrystals in PVA matrix the characteristic peaks of PVA are completely lost, which suggests that the chemical structure of PVA has changed completely. Spectra of SiC-PVA nanocomposite film [Figure 5(A)] display four intense bands at 786 cm^{-1}, 917 cm^{-1}, 1362 cm^{-1}, and 1604 cm^{-1}. The bands at 786 cm^{-1} and 917 cm^{-1} corresponds to the transverse optical (TO) and longitudinal optical (LO) modes of the SiC nanocrystals[29] while the bands at 1362 cm^{-1} and 1604 cm^{-1} are disorder D bands and graphite like G band, respectively. The D-band corresponds to the breathing mode of *k*-point phonons of A_{1g} symmetry while the G-band represents first-order scattering process of sp^2 carbons in E_{2g} stretching mode. The D band is forbidden in perfect graphite and only becomes active in the presence of disorder.

The FWHMs of TO and LO bands lie in the range of 21–35 cm^{-1}, suggesting that SiC nanocrystals contain defects and stacking faults, which may lead to the shifting and variation in the band positions of the TO and LO modes. XRD analysis also points towards the presence of stacking faults in SiC nanocrystals.

It can also be discerned from Figure 5(A) that the spectrum of 1 wt % SiC-PVA nanocomposite film solely shows bands corresponding to SiC nanocrystals and bands related to PVA are not observed. This screening of bands may be ascribed to the use of 532 nm excitation wavelength that matches better with SiC

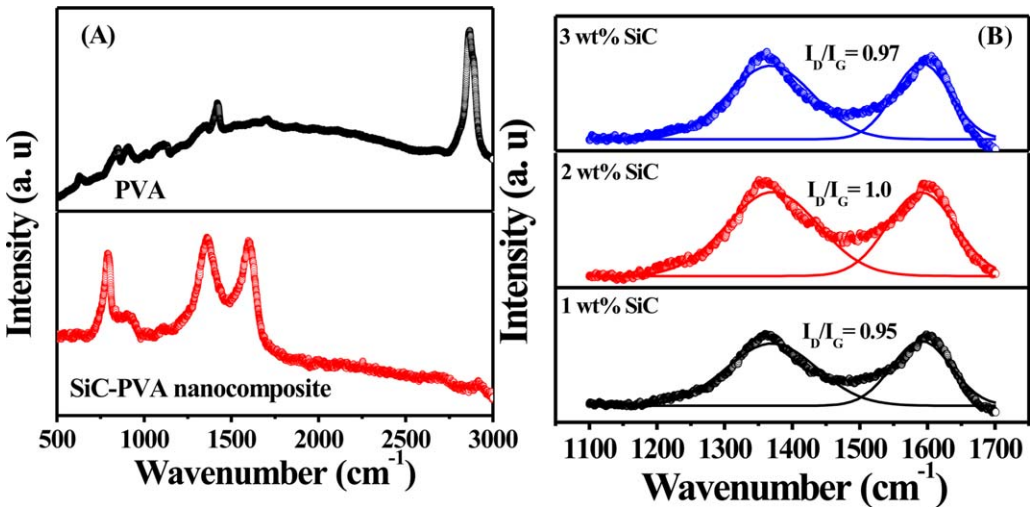

Figure 5. (A) RAMAN spectrum of PVA and 1 wt % SiC-PVA nanocomposite. (B) Deconvoluted RAMAN spectrum of SiC-PVA nanocomposite. [Color figure can be viewed in the online issue, which is available at wileyonlinelibrary.com.]

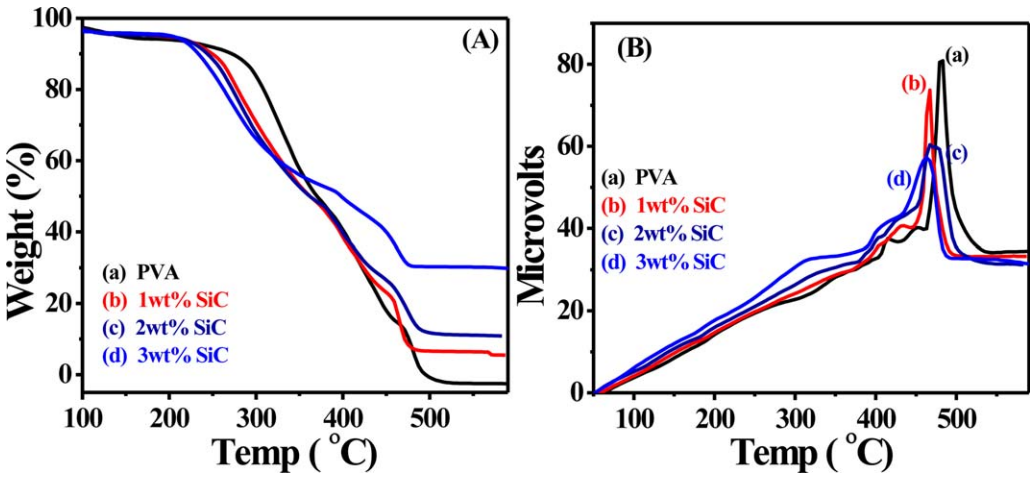

Figure 6. (A) TGA and (B) DTA curves of (a) PVA and SiC-PVA nanocomposite films containing (b) 1 wt % (c) 2 wt % (d) 3 wt % SiC nanocrystals. [Color figure can be viewed in the online issue, which is available at wileyonlinelibrary.com.]

vibrations than with PVA.[30] The spectra of 2 wt % and 3 wt % SiC-PVA nanocomposite films show similar features and are not presented here.

The ratio of relative intensities of the D and G bands (I_D/I_G) is a measure of the extent of disorder present in the SiC nanocrystals.[30] For analyzing structural changes in nanocomposite films, Raman spectra were deconvoluted with Gaussian fit after background subtraction. The deconvoluted *D* and *G* bands are shown in Figure 5(B). From Figure 5(B) I_D/I_G is 0.95 for 1 wt % SiC-PVA nanocomposite film and is 0.97 for 3 wt % SiC-PVA nanocomposites film. I_D/I_G ratio increases slightly with increasing concentration of SiC nanocrystals. This marginal increase in I_D/I_G ratio show that after the addition of SiC nanocrystals in PVA matrix the disorder increases.

Thermal Analysis

TG/DTA is an effective tool for determining the thermal stability of the material. In this process, a material is decomposed by heat which causes bonds within the molecule to break. Figure 6(A) shows the TGA curve for PVA and SiC-PVA nanocomposite films with different concentration of SiC nanocrystal and Figure 6(B) represents their derivative in terms of the weight loss as a function of temperature. It is clear from Figure 6(A) that the thermal degradation of SiC-PVA nanocomposite films is different from that of pure PVA. It can be discerned from Figure 6(A) that, the maximum decomposition temperature (T_{max}) for PVA film is ~275°C and it reduces to ~214°C for the nanocomposite film containing 3 wt % SiC nanocrystals. Thus the introduction of SiC nanocrystals in PVA matrix shifts the onset of thermal decomposition to lower temperatures. Moreover, all the samples show a small mass loss (~5–10%) for the first decomposition stage (~50–210°C) and more significant mass loss (~60–90%) for the second stage (~210–500°C). The lower value of percentage mass loss in the first stage is presumably due to the evaporation of bound water molecules. At low temperatures (<400°C) PVA displays better thermal stability than SiC-PVA nanocomposite films, as the presence of SiC nanocrystals accelerates the degradation of PVA. This observation has been reported as the Hofmann elimination reaction, where nanoparticles act as a catalyzer toward the degradation of the polymer matrix.[31,32]

In the second stage, i.e., the temperature range of ~210−500°C, PVA [Figure 6(A) curve a] decomposes with appreciable mass loss as it vaporizes. This degradation of PVA with maximum mass loss is accompanied by an exothermic peak at a temperature of ~480°C, as can be seen in DTA curve. At a temperature of 494°C a mass loss of 90% is observed for PVA, 82% for 1 wt %, 80% for 2 wt % and 64% for 3 wt % SiC nanocrystal concentration in PVA matrix. This decrease in mass loss with increase in concentration of SiC nanocrystals in PVA matrix may be due to the restricted mobility of polymer chains and may lead to decrease in crystallinity of the nanocomposites films. The nanocomposite film with 3 wt % SiC leaves a residue also known as char of about 30% of initial material; however, PVA leaves no residue. This enhancement of the char formation can be ascribed to the high heat resistance exerted by SiC nanocrystals. It is well quoted in literature that the thermal stability of PVA matrix is highly influenced by the type of filler being incorporated. For example, sepiolite and HT Sepiolites[33] and silver nanoparticles[34] improve the thermal stability of PVA, on the other hand magnetite nanoparticles[35] decreases the thermal stability of PVA, whereas in the presence of montmorillonite[36] the thermal stability of PVA does not change. The increase in char yield is an indication of the potency of flame retardation of polymers. Therefore, higher the amount of residual char after combustion, lower is the amount of combustible material for perpetuating the flame and greater is the degree of flame retardency. Alamari *et al.*[3] showed that after the addition of 3 and 5 wt % n-SiC in neat epoxy resulted in increase in char residue from 13.1 to 13.2% and 14.0%, respectively and in the present studies addition of 3 wt % SiC nanocrystals leaves a residue of about 30% of initial material. Thus addition of SiC nanocrystals in PVA matrix increases its thermal stability.

Electrical Characterization

To understand the conduction mechanism prevalent in SiC-PVA nanocomposite films, the charge transport measurements were carried out in metal-nanocomposite-metal sandwich structure.

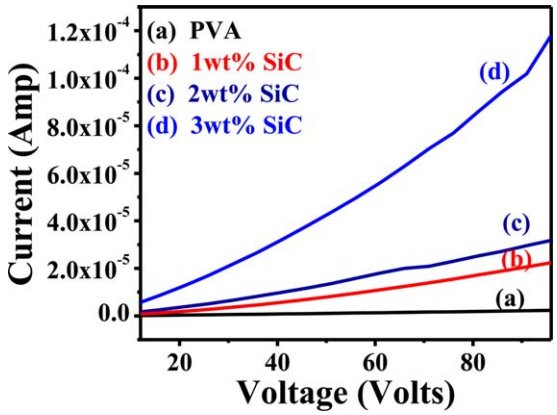

Figure 7. Current-Voltage variation of (a) PVA and SiC-PVA nanocomposite films containing (b) 1 wt % (c) 2 wt % (d) 3 wt % SiC nanocrystals. [Color figure can be viewed in the online issue, which is available at wileyonlinelibrary.com.]

Figure 7 shows the current–voltage characteristics of PVA and SiC-PVA nanocomposite films. It is clear from figure that the conductivity of PVA increases after incorporation of SiC nanocrystals into PVA matrix. Addition of 3 wt % of SiC nanocrystals to PVA matrix increases the conductivity by 5 orders of magnitude. Figure 7 also depicts the nonlinear nature of *I-V* curves for nanocomposites films. In order to explain these nonlinear *I-V* characteristics four different conduction mechanisms were considered: variable range hopping, Schottky emission, Poole-Frenkel emission and space charge-limited conduction (SCLC).

In the hopping model, charge may hop between adjacent sites as a result of an external electric field and current is expressed as[37]

$$I \sim \sinh \mathrm{AV}/\mathrm{k_B T} \tag{3}$$

where A is a constant that depends on the hopping distance and the length of the sample. In SCLC mechanism, the injected carriers are larger than the intrinsic carrier present in the sample, which create a space-charge region near the interface and is responsible for the bulk limited SCLC.[38]

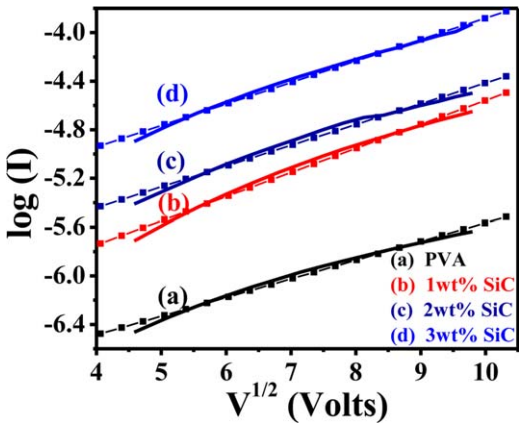

Figure 8. Plot of ln(I) vs. $V^{1/2}$ for PVA and SiC-PVA nanocomposite films. [Color figure can be viewed in the online issue, which is available at wileyonlinelibrary.com.]

Conduction in nanocomposite films may also be due to charge carriers that are released by thermal activation over the coulombic potential barrier that is decreased by the applied electric field. The physical nature of such a potential barrier can be interpreted either by Schottky mechanism or by Poole-Frenkel mechanism. In Schottky mechanism the current is due to the transition of electrons over the barrier between the cathode (metal electrode) and nanocomposite film. It is an electrode limited process. In Poole-Frenkel mechanism the emission of charge carriers trapped in the defect centers, contributes to the conduction process.[39,40] Hence it is a bulk limited process.

For the Schottky effect the current–voltage expression is given by:[41]

$$I \sim AT^2 \exp\left(-\phi s/kT\right) \exp\left(\beta_s V^{\frac{1}{2}}/kT\right) \tag{4}$$

and for the Poole–Frenkel effect current–voltage expression is given by:

$$I \sim V \exp\left(\beta_{PF} V^{\frac{1}{2}}/kT\right) \tag{5}$$

In these expressions A ($=1.2 \times 10^6$ Am^{-2}) is the Richardson constant, T is the absolute temperature, (φ_s) is the Schottky barrier height at the injecting electrode interface, k is Boltzmann's constant. β_s and β_{PF} are, respectively, the Schottky and Poole–Frenkel field-lowering coefficients.

Each of these mechanisms was evaluated by comparing the measured *I-V* curves with curve fits obtained using different models. For SCLC mechanism to occur slope of log$I$ - log$V$ graph should be greater than 2 but in the present case the slope is less than 2 so this conduction mechanism was ruled out.[42] Also the results of hopping model were not a perfect fit to the experimental data so this mechanism was also ruled out. Hence, the conduction mechanism involved in SiC-PVA nanocomposite films can either be Schottky or Poole-Frenkel mechanisms.

To determine the exact charge transport mechanism, graphs between log I vs. $V^{1/2}$ (for Schottky mechanism) and log (I/V) vs. $V^{1/2}$ (for Poole-Frenkel mechanism) were plotted.[43] The measured values for Schottky mechanism as shown in Figure 8 were linear when compared with plots obtained from Poole-Frenkel mechanism, and the fitting was reasonably good as the correlation coefficient (R) for the straight lines of the best fit comes out to be 0.99. Hence, it can be concluded that the conduction mechanism which is responsible for the substantial increase in the conductivity of SiC-PVA nanocomposite films is Schottky mechanism.

Similar studies have been consummated by Tkaczyk using SiC nanoparticles in Polybutadiene matrix. They observed a substantial increase in conductivity with addition of 5 wt % SiC nanoparticles in Polybutadiene matrix and have concluded that hopping and Poole-Frenkel conduction mechanisms are chiefly responsible for increased conductivity of Polybutadiene.[11] There are numerous reports in literature which show an increase in conductivity of PVA after incorporation of Ag, Cu, I, etc. nanoparticles.[44–47] By far no studies have been carried out to establish conduction mechanism in SiC-PVA nanocomposite.

CONCLUSIONS

Nanocomposite films of PVA doped with different concentration of SiC nanocrystals were formed by solution-casting method. Thermal, structural and electrical properties of PVA matrix were significantly altered by the presence of SiC nanocrystals. Structural characterization of the formed nanocomposites films using XRD, FTIR, and Raman spectroscopy shows SiC nanocrystals interacts with the PVA matrix and results in an increase in disorder and reduced crystallinity. Sizes obtained from TEM and XRD are in good agreement. TG/DTA studies had revealed that addition of 3 wt % SiC nanocystals in PVA increases the thermal stability as char yield is increased by 30% as compared with that of PVA matrix. *I-V* studies indicate that the conductivity of PVA increase five times with the addition of 3 wt % SiC nanocystals in PVA matrix and Schottky mechanism is found to be the dominant conduction mechanism responsible for this increase. Our results also indicate that such nanocomposites offer good opportunities for the use in detectors, filters, varistors, etc.

ACKNOWLEDGMENTS

The authors are grateful to Dr. Sanjeev Arora, Department of Chemistry, Kurukshetra University, Kurukshetra, India, for TGA/DTA facility, Prof Per Morgen, from Department of Physics, Chemistry and Pharmacy, University of Southern Denmark, Odense, Denmark, for SEM and Raman facility. One of the authors (IS) is thankful to UGC for UGC-BSR fellowship.

REFERENCES

1. Yang, W.; Yi, R.; Hui, S.; Xu, Y.; Cao, X. *J. Appl. Polym. Sci.* **2013**, *127*, 3891.
2. Dong, Y. *J. Appl. Poly. Sci.* **2012**, *127*, 3933.
3. Alamri, H.; Low, I. M. *J. Appl. Poly. Sci.* **2012**, *126*, E221.
4. Shi, S. L.; Xu, S. J.; Wang, X. J.; Chen, G. H. *Thin Solid Films* **2006**, *495*, 404.
5. Liu, L.; Yiu, Y. M.; Sham, T. K.; Zhang, L.; Zhang, Y. *J. Phys. Chem. C* **2010**, *114*, 6966.
6. Martensson, E.; Gafvert, A. U.; Onneby, C. *J. Appl. Phys.* **2001**, *90*, 2870.
7. Niihara, K. *J. Ceram. Soc.* **1991**, *99*, 945.
8. Rodgers, R. M.; Mahfuz, H.; Rangari, V. K.; Chisholm, N.; Jeelani, S. *Macromol. Mater. Eng.* **2005**, *290*, 423.
9. Guo, Z.; Kim, T. Y.; Lei, K.; Pereira, T.; Sugar, J. G.; Hahn, H. T. *Compos. Sci. Technol.* **2008**, *68*, 164.
10. Chisholm, N.; Mahfuz, H.; Rangari, V. K.; Ashfaq, A.; Jeelani, S. *Comp. Struct.* **2005**, *67*, 115.
11. Tkaczyk, S. W. *Physica E* **2011**, *43*, 1179.
12. Dash, S.; Swain, S. K. *Carbohydr. Polym.* **2013**, *97*, 758.
13. DeMerlis, C. C.; Schoneker, D. R. *Food Chem. Toxicol.* **2003**, *41*, 319.
14. Vivekchand, S. R. C.; Ramamurty, U.; Rao, C. N. R. *Nanotechnology* **2006**, *17*, S344.
15. Zhang, J. X.; Jiang, D. L.; Tan, S. H.; Gui, L. H.; Ruan, M. L. *J. Mater. Res.* **2002**, *17*, 2019.
16. Dhiman, R.; Johnson, E.; Skou, E. M.; Morgen, P.; Andersen, S. M. *J. Mater. Chem. A* **2013**, *1*, 6030.
17. Dhiman, R.; Petrunin, V.; Rana, K.; Morgen, P. *Ceram. Int.* **2011**, *37*, 3281.
18. PAX-ray Powder Diffraction File JCPDS-ICDD (Joint Committee on Powder Diffraction Standard- International Centre for Diffraction Data 1999. File PDF No. 29–1129.
19. Wang, Y.; Iqbal, Z.; Mitra, S. *Carbon* **2006**, *44*, 2804.
20. Mavinakuli, P.; Wei, S.; Wang, Q.; Karki, A. B.; Dhage, S.; Wang, Z.; Young, D. P.; Guo, Z. *J. Phys. Chem. C* **2010**, *114*, 3874.
21. Cullity, B. D. Elements of X-Ray Diffraction; Addison Wesley Pub. Co: U.S.A., **1978**.
22. Dunn, A. S. In Polyvinyl Alcohol: Developments; Finch, C. A., Ed.; Wiley: London, **1992**.
23. Andrade, G. I.; Stancioli, E. F. B.; Mansur, A. A. P.; Vasconcelos, W. L.; Mansur, H. S. *J. Mater. Sci.* **2008**, *43*, 450.
24. Tawansi, A.; Zidan, H. M.; Oraby, A. H.; Dorgham, M. E. *J. Phys. D: Appl. Phys.* **1998**, *31*, 3428.
25. Majewski, P.; Choudhury, N. R.; Spori, D.; Wohlfahrt, E.; Wohlschloegel, M. *Mater. Sci. Eng. A* **2006**, *434*, 360.
26. Che, J.; Wang, X.; Xiao, Y.; Wu, X.; Zhou, L.; Yuan, W. *Nanotechnology* **2007**, *18*, 135706.
27. Li, J. P.; Steckl, A. J.; Golecki, I.; Reidinger, F.; Wang, L.; Ning, X. J.; Pirouz, P. *Appl. Phys. Lett.* **1993**, *62*, 3135.
28. Tripathi, J.; Keller, J. M.; Das, K.; Tripathi, S.; Shripathi, T. *J. Phys. Chem. Solids* **2012**, *73*, 1026.
29. Wieligor, M.; Wang, Y.; Zerda, T. W. *J. Phys: Condens. Matter* **2005**, *17*, 2387.
30. Peregrino, P. P.; Sales, M. J. A.; daSilva, M. F. P.; Solerc, M. A. G.; daSilva, L. F. L.; Moreira, S. G. C.; Paternoa, L. G. *Carbohydr. Polym.* **2014**, *106*, 305.
31. Madaleno, L.; Thomsen, J. S.; Pinto, J. C. *Compos. Sci. Technol.* **2010**, *70*, 804.
32. Ismail, H.; Pasbakhsh, P.; Fauzi, M. N. A.; Bakar, A. A. *Polym. Test.* **2008**, *27*, 841.
33. Alkan, M.; Benlikaya, R. *J. Appl. Poly. Sci.* **2009**, *112*, 3764.
34. Mbhele, Z. H.; Salemane, M. G.; Van Sittert, C. G. C. E.; Nedeljkovic', J. M.; Djokovic', V.; Luyt, A. S. *Chem. Mater.* **2003**, *15*, 5019.
35. Kumar, R. V.; Koltypin, Y.; Cohen, Y. S.; Aurbach, D.; Palchik, O.; Felner, I.; Gedanken, A. *J. Mater. Chem.* **2000**, *10*, 1125.
36. Strawhecker, K. E.; Manias, E. *Chem. Mater.* **2000**, *12*, 2943.
37. Choueib, M.; Ayari, A.; Vincent, P.; Perisanu, S.; Purcell, S. T. *J. Appl. Phys.* **2011**, *109*, 073709.
38. Cheong, K. Y.; Moon, J. H.; Kim, H. J.; Bahng, W.; Kim, N. K. *J. Appl. Phys.* **2008**, *103*, 084113.
39. Simmons, J. G. *Phys. Rev.* **1967**, *155*, 657.
40. Mansour, S. A.; Al-Ghoury, M. E.; Shalaan, E.; El Eraki, M. H. I.; Abdel-Bary, E. M. *J. Appl. Poly. Sci.* **2010**, *116*, 3134.

41. Sze, S. Physics of Semiconductor Devices; Wiley: New York, **1983**.

42. Chawla, M.; Shekhawat, N.; Aggarwal, S.; Sharma, A.; Nair, K. G. M. *J. Appl. Phys.* **2014**, *115* 184104.

43. Mahrous, S.; Hanfy, T. A. *Curr. Appl. Phys.* **2004**, *4*, 461.

44. Devi, C. U.; Sharma, A. K.; Rao, V. V. R. N. *Mater. Lett.* **2002**, *56*, 167.

45. Rozra, J.; Saini, I.; Sharma, A.; Chandak, N.; Aggarwal, S.; Dhiman, R.; Sharma, P. K. *Mater. Chem. Phys.* **2012**, *134*, 1121.

46. Saini, I.; Rozra, J.; Chandak, N.; Aggarwal, S.; Sharma, P. K.; Sharma, A. *Mater. Chem. Phys.* **2013**, *139*, 802.

47. Kulanthaisami, S.; Mangalaraj, D.; Narayandass, S. K. *Eur. Polym. J.* **1995**, *31*, 969.